CO binding to heme proteins: A model for barrier height distributions and slow conformational changes

Noam Agmon and J. J. Hopfield

Citation: The Journal of Chemical Physics **79**, 2042 (1983); doi: 10.1063/1.445988
View online: http://dx.doi.org/10.1063/1.445988
View Table of Contents: http://scitation.aip.org/content/aip/journal/jcp/79/4?ver=pdfcov
Published by the AIP Publishing

CO binding to heme proteins: A model for barrier height distributions and slow conformational changes[a)]

Noam Agmon[b)] and J. J. Hopfield[c)]

The Division of Chemistry, Calfornia Institute of Technology, Pasadena, California 91125
(Received 14 December 1982; accepted 4 May 1983)

A model for the dependence of the potential energy barrier on a "protein coordinate" is constructed. It is based on a two dimensional potential energy surface having as variables the CO–iron distance and a conceptual protein coordinate. The distribution of barrier heights observed in kinetics follows from an initial Boltzmann distribution for the protein coordinate. The experimental nonexponential rebinding kinetics at low temperatures or large viscosities (when the protein coordinates can be assumed "frozen") can be fit with a simply parametrized energy surface. Using the same energy surfaces and the theory of bounded diffusion perpendicular to the reaction coordinate, we generate (in qualitative agreement with experiment) the survival probability curves for larger diffusivity, when the constraint on the protein coordinate is relaxed. On the basis of our results, the outcomes of new experiments which examine the concepts underlying the theory can be predicted.

I. INTRODUCTION

Heme proteins are perhaps the best understood class of protein molecules.[1] They are the most obvious candidate for trying to understand the effect of the overall protein on the "local" chemistry of small ligand binding. The kinetics of ligand binding to heme molecules has been studied[2,3] over a large range of temperatures and solvent viscosities. In a typical experiment[2] a sample of bound heme–ligand in a solvent saturated with ligand is cooled to the desired termperature, the ligand is flashed off by a strong light flash (of duration ~ 1 μs; the ns regime is just recently being investigated[4]) and the fraction of unbound heme is followed as a function of time (from 2 μs to a few seconds) by a monitoring beam in the Soret band.

At low temperatures, the same ligand molecule previously on a given heme recombines with that heme. The "survival probability" measured as above shows a power law time dependence, in contrast to the familiar exponential kinetics of elementary unimolecular reactions. As the temperature is increased the kinetics gradually becomes exponential. A similar transition from power law at high viscosities (small diffusivity) to exponential at low viscosities is observed at constant temperature as a function of solvent viscosity. But in spite of the viscosity dependence, the reaction rate does not tend to zero at high viscosities, in contrast to Kramers' model.

The observed nonexponential kinetics is apparently related to the fact that these large macromolecules have many conformations[6(a)] which can differ substantially in barrier height for ligand rebinding. If at low temperatures the rate of changing between such conformations is slow, an individual molecule will not be able to average the activation barrier over all conformations, resulting in an experimental observation of a distribution of barrier heights[2] instead of a sharp activation energy. Experiments have been fit by such distributions,[2] but a microscopic physical model from which these can be generated has not been proposed.

At higher temperatures (and lower viscosities) the observed kinetics was explained[2] in terms of sequential barriers. At the highest temperature, ligand escape into solution becomes dominant and the kinetics is exponential and bimolecular. The above experimental results spurred additional theoretical work,[7–12] in an effort to determine the ligand's path from the "heme pocket" into solution[7] and explain the temperature[9,10] and viscosity[11,12] dependence of the rate constants.

The present work has two objectives. First, a physical model for distribution of barrier heights for CO binding is constructed and fitted to the low temperature results. The model involves an energy surface for rebinding which depends on both the heme–ligand and the protein coordinates. Such a model provides a conceptual and quantitative framework for understanding the origin of such distributions. In addition, it is a significant guide to constructing new experiments.

Second, the theory of bounded diffusion perpendicular to the reaction coordinate[13] is used to project the kinetic results to higher temperatures (or lower viscosities). We observe that the turnover to exponential kinetics can be an effect of *parallel* reactions from the different conformations (even without invoking a *sequential*[2] kinetic scheme) and that a non-Kramers dependence on viscosity can result from diffusion perpendicular to the reaction coordinate (without the need to invoke a relation of "internal" and "external" viscosities[11]).

II. THEORY

The physical picture for geminate (unimolecular) ligand binding from the heme pocket is as follows: For each protein configuration x there is a different binding rate constant $k(x)$. At low temperatures (or high viscosities) when the protein coordinate is "frozen," each protein molecule i has a particular value x_i of its co-

[a)]Supported in part by National Science Foundation grant No. DMR-8107494.
[b)]Chaim Weizmann Fellow for 1982 in the Division of Chemistry. Permanent address: Department of Physical Chemistry, The Hebrew University, Jerusalem 91904, Israel.
[c)]Divisions of Chemistry and Biology. Also, Bell Laboratories, Murray Hill, NJ 07974.

 0021-9606/83/162042-12$02.10

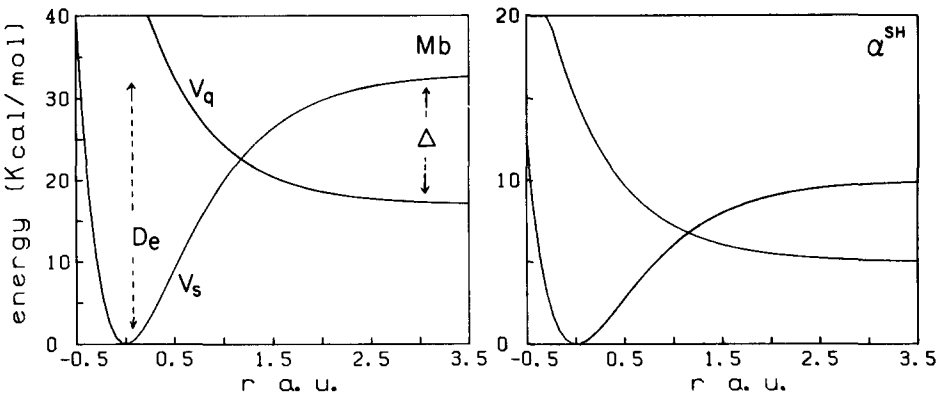

FIG. 1. Potential energy as a function of Fe–CO distance for the two spin states [Eqs. (2) and (3)] for myoglobin (Mb) and α heme. (Note the change in scale). The curves for β heme and protoheme resemble more those of α heme. D_e and Δ given in Table I. $\beta = 1.5$ a.u.$^{-1}$ is a reasonable number, though it has no effect on the results.

ordinate, and is an independent chemical species with a rate constant $k(x_i)$. The observed recombination is then an average over all the molecules i. Higher temperature (or lower viscosities) allow an additional process of x variation within a molecule to take place. This results in a variation of barrier height with time according to the time dependence of x and the x dependence of the barrier height, as determined from the low temperature kinetics.

The theory consists of three parts. The first is a model for $k(x)$ calculated through evaluating the dependence of the barrier height $V^{\ddagger}$ on x for ligation at fixed x. The second part uses the distribution of x and thus of $V^{\ddagger}$ to explain the low temperature results. The last part solves the x coordinate dynamics for the higher temperature kinetics.

A. Barrier heights

At least two degrees of freedom must be considered. One is the reaction coordinate r which can be taken as the Fe-ligand distance. The other is a protein coordinate x describing the overall effect of the surroundings (protein or solvent) on the heme ring. Of course, a fuller model might include many more degrees of freedom, but we prefer the simplest model possible. It suffices to gain understanding of the central physical phenomena involved, and the present amount of experimental detail does not justify the introduction of additional parameters and assumptions. If the potential energy surface $V(r, x)$ for the heme molecule is known the kinetic rebinding problem can be described as follows: At low temperatures, a given protein molecule i has an internal coordinate x_i which is frozen during the entire rebinding process, and which has whatever initial value pertained to that molecule just before the flash photolysis. For such a molecule, the entire rebinding kinetics can be described using transition state theory on the coordinate r for x_i is fixed.

$$k(x_i) = A \exp[V^{\ddagger}(x_i)/k_B T] , \tag{1}$$

where k_B is Boltzmann's constant, T is the absolute temperature and the preexponent A is assumed to be temperature (and viscosity) independent, i.e., we neglect the difference between potential and free energies. $V^{\ddagger}$ can in turn be determined from the energy surface $V(r, x_i)$. (At this point, we can drop the subscript i, which is only of pedagogic value in describing what is being done.) Thus, $V^{\ddagger}(x)$ is defined as the barrier height for constant x.

We next construct a model potential $V(r, x)$ for CO binding. (For CO binding, probably only two spin states are involved in contrast to O_2 binding, where one has to consider three spin states.[15]) The bound (six coordinated) iron is in strong ligand field and the total spin is $S = 0$ (singlet). We model this potential by a Morse curve

$$V_s(r) = D_e [\exp(-2\beta r) - 2\exp(-\beta r)] , \tag{2}$$

where r is the deviation from the equilibrium Fe–CO bond length, D_e is the well depth, and β determines the curvature. In the unbound (five coordinated) state the low ligand field results in a total spin $S = 2$ (quintet) and a repulsive potential. This we take as a simple exponential repulsion

$$V_q(r) = D_e \exp(-\beta r) - \Delta \tag{3}$$

shifted by Δ. (There is some controversy surrounding Δ with cited values for it smaller than $k_B T$[14] or as large as 1 eV.[15])

The two spin functions are shown in Fig. 1. In the intersection of the two curves, degeneracy is removed by a transition matrix element which determines whether the reaction is adiabatic or nonadiabatic.[16] It also determines the preexponential constant A in $k(x)$, which we do not try to calculate but take as a free parameter.

The protein dependence of the potential function is coupled to the ligation process through the fact that the ligated and unligated hemes have different geometries. For example, on binding a strong-field ligand, the hemes in hemoglobin[1] or model systems[17] tend to go from domed (with the Fe atom out of plane toward the fifth ligand) to planar. The planar geometry is preferred for low spin.

The potential along the protein coordinate is modeled as harmonic with a weak force constant describing the effect of fluctuations in many atomic degrees of freedom.[6] The equilibrium value for x is different for the two spin states with a shift of x_0. (In principle, the force constants may also be different for the two spin states, but this is a secondary effect and we prefer not to introduce an additional parameter.) Since the spin mixing matrix ele-

ment should be weak, we find

$$V(r,x) = \text{the lesser of} \begin{cases} V_s(r) + \frac{1}{2} f(x-x_0)^2 \\ V_q(r) + \frac{1}{2} f x^2 \end{cases} . \quad (4)$$

Some typical surfaces are shown in Fig. 2. The well at upper left corresponds to bound heme-CO ($S=0$) and that at lower right to deligated heme ($S=2$). The crestline where the two different parts of Eq. (4) intersect is also evident. For any value of x, the intersection is at a different value of r, denoted by $r^{\ddagger}(x)$. The barrier height as a function of x is calculated from the energy at the intersection

$$V^{\ddagger}(x) \equiv V(r^{\ddagger}, x) - V(\infty, x) = D_e \exp(-\beta r^{\ddagger}) \quad (5)$$

and is

$$V^{\ddagger}(3 - V^{\ddagger}/D_e) = \tfrac{1}{2} f x_0 (x_0 - 2x) + \Delta . \quad (6)$$

The dependence of $V^{\ddagger}(x)$ on x for some typical cases is shown in Fig. 3. It can be seen that $V^{\ddagger}(x)$ is almost linear [$V^{\ddagger}(x)/D_e \ll 3$ in Eq. (6)]. Hence, only two independent combinations of the four parameters (D_e, f, x_0, Δ) determine the value of $V^{\ddagger}$, namely, fx_0^2 and $\frac{1}{2} fx_0^2 + \Delta$ (D_e has only a minor effect on $V^{\ddagger}$, and β none at all). Finally, the rate constant is given by Eq. (1).

B. Distribution of barrier heights

At low temperatures (or high viscosities) the protein coordinate is assumed "frozen." The fraction $p^0(x)$ of heme molecules initially in a conformation x, react with a rate constant $k(x)$ without changing their x value during either flash or reaction. Hence, $p^0(x)$ can be taken as the distribution of the bound heme, before the ligand is flashed off, when we assume that a state of equilibrium prevailed

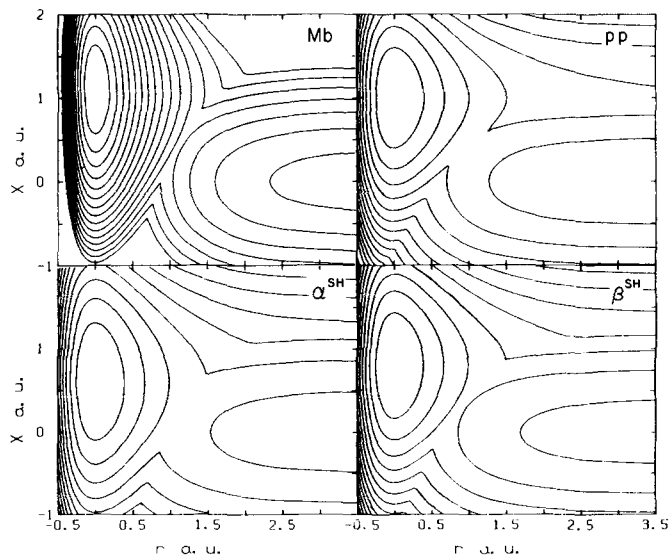

FIG. 2. Potential energy surfaces as a function of Fe–CO distance r and protein coordinate x [cf. Eq. (4)]. Relevant parameters (D_e, Δ, f, x_0) given in Table I (the value of $\beta = 1.5$ a.u.$^{-1}$ has no effect on the final results). Equipotential contours spaced 2 kcal/mol with zero energy in the bottom of the Fe–CO well. The curves $V_s(r)$ and $V_q(r)$ shown in Fig. 1 are cuts at $x = x_0$ and $x = 0$, respectively.

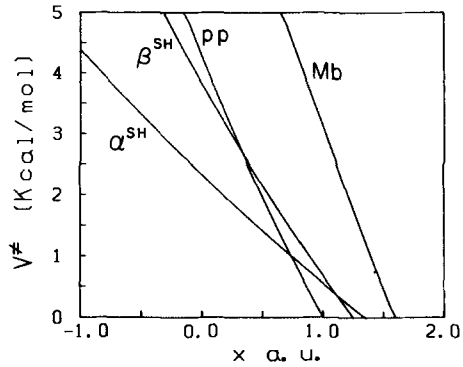

FIG. 3. Barrier height as a function of protein coordinate, Eq. (6). Relevant parameters (D_e, Δ, f, x_0) from Table I.

$$p^0(x) = (f/2\pi k_B T_0)^{1/2} \exp\left[-\frac{f(x-x_0)^2}{2k_B T_0}\right] . \quad (7)$$

The temperature T_0 is the temperature at which equilibrium of the bound heme–ligand was achieved. It is not necessarily equal to T, the sample's temperature during experiment, since both the external medium and probably the protein interior undergo liquid–glass transitions when cooled. In applications, we take T_0 to be the freezing temperature of the sample T_f for $T < T_f$ but equal to T if $T > T_f$.

The distribution of barrier heights $p(V^{\ddagger})$ follows from a change of variable in Eq. (7), namely,

$$p(V^{\ddagger}) = p^0(x(V^{\ddagger}))\,|dx/dV^{\ddagger}| , \quad (8)$$

where from Eq. (6) we find that

$$dV^{\ddagger}/dx = fx_0/(2V^{\ddagger}/D_e - 3) . \quad (9)$$

Since [cf. Eqs. (6) and (7)] $V^{\ddagger}$ is almost linear in x, $p(V^{\ddagger})$ is approximately a Gaussian with a peak at $V^{\ddagger}(x_0)$.

The "survival probability" (the probability that a heme molecule does not react up to time t) $Q(t)$, which is the quantity accessible experimentally, is then

$$Q(t) = \int_{-\infty}^{\infty} \exp[-k(x)t]\,p^0(x)\,dx = \int_0^{\infty} \exp[-k(V^{\ddagger})t]\,p(V^{\ddagger})dV^{\ddagger} . \quad (10)$$

C. Coupling of diffusion and reaction

By increasing the temperature (or the diffusivity), the constraint $x = \text{const.}$ is relaxed. The unbound protein can change its configuration in addition to reacting. This configurational change in coordinate x is assumed to be slow compared to the preexponential factor A in Eq. (1), and to be diffusive (in contrast to the coordinate r, which is a Hamiltonian or "ballistic" motion). The random motion along x can then be described by a diffusion (Smoluchowski) equations[5(b)]:

$$\partial p(x,t)/\partial t = D\,\partial^2 p/\partial x^2 + \frac{D}{k_B T}\frac{\partial}{\partial x}\left(p\frac{\partial V}{\partial x}\right) - k(x)\,p , \quad (11)$$

where the diffusion constant D is inversely proportional to the "viscosity" (not necessarily equal to the viscosity in solution). The term $-k(x)p$ represents the recombination events.

TABLE I. Parameters[a] for binding of CO to heme molecules.

Heme[b]	D_e[c]	Δ[c]	f[d]	x_0[e]	T_0[f]	log$A$[g]	Reference[h]
Mb	33	16	14	1.1	220	8.7	2a, 3
α^{SH}	10	5	8	0.6	200	8.7	2b
β^{SH}	10	6.8	10	0.8	200	9.8	2b
pp	10	5.5	11	1.0	220	10.5	2c
hp	12	8.6	17	1.2	200	9.0	2d

[a]Not necessarily "best fit" parameters.
[b]Abbreviations as in text.
[c]In kcal/mol [cf. Eqs. (2) and (3)].
[d]In kcal/(mol a.u.^{2}) [cf. Eq. (4)].
[e]In a.u., 1 a.u. = 0.569 Å [cf. Eq. (4)].
[f]In degrees Kelvin [cf. Eq. (7)].
[g]A in s^{-1}; logarithm base 10 [cf. Eq. (1)]. The values used in Ref. 2(a) and (b) are 8.7, 8.6, and 9.4 for Mb, α^{SH} and β^{SH}, respectively.
[h]Reference for experimental results.

Unlike the conventional approach,[5(a)] diffusion here is in a degree of freedom other than the reaction coordinate r. This we term "diffusion perpendicular to the reaction coordinate." It is characterized mathematically by a slowly varying $k(x)$. In addition, the potential along x, $V(x) = \frac{1}{2} fx^2$, restricts the random motion to the vicinity of $x = 0$ resulting in "bounded diffusion."

The solution[13] for $p(x,t)$ [Eq. (11)] under the above conditions enables one to calculate the survival probability

$$Q(t) = \int_{-\infty}^{\infty} p(x,t)\,dx \ . \tag{12}$$

In the low temperature limit $D \to 0$, $p(x,t)$ becomes $p^0(x)\exp[-k(x)t]$, and Eq. (12) agrees with Eq. (10). At higher temperatures or lower viscosities one must compute the time dependent $p(x,t)$ by direct integration of Eq. (11) at low D and by the eigenvalue technique otherwise.[13] The larger D, the less terms contribute to the eigenvalue expansion. Eventually, only the smallest eigenvalue λ_0 survives. It can be evaluated[13] from a linear approximation to $V^{\ddagger}$ [$3V^{\ddagger} \cong \Delta + \frac{1}{2} fx_0^2 - fx_0 x$, cf. Eq. (6)], and the equilibrium distribution p^{eq}, in reagents [replacing $x - x_0$ by x in Eq. (7)]. The result for very large D,

$$\lambda_0 \underset{D\to\infty}{\longrightarrow} \int_{-\infty}^{\infty} p^{eq}(x)\,k(x)\,dx = A(f/2\pi k_B T)^{1/2}$$

$$\times \int_{-\infty}^{\infty} \exp(-V^{\ddagger}/k_B T)\exp(-fx^2/2k_B T)\,dx \cong A\,\exp(-E_A/k_B T) \tag{13}$$

is in an Arrhenius form, with an activation energy given by

$$E_A = \tfrac{1}{3}[\Delta + \tfrac{1}{6} fx_0^2] \ . \tag{14}$$

The temperature dependence of the higher eigenvalues in the large D limit is approximately

$$\lambda_n = nDf/k_B T \ , \quad n = 1, 2\ldots \ . \tag{15}$$

Only the lowest eigenfunction is everywhere positive like an ordinary probability distribution. The higher eigenfunctions have n nodes and populations which tend to zero as $D \to \infty$. The full theory of bounded diffusion is given in Ref. 13.

III. RESULTS AND DISCUSSION

The model for barrier height dependence on protein coordinate is used to explain low temperature or high viscosity ("frozen" protein coordinate) and high temperature or low viscosity ("relaxed" protein coordinate) kinetics. The model is limited at present to the simpler case of CO binding, where only two spin states are important ($S = 1$ is higher in energy). The (ferrous) hemes for which we carry out the calculations are[2] sperm whale myoglobin (Mb), α and β subunits of human hemoglobin (α^{SH} and β^{SH}), protoporphyrin IX (protoheme; pp) and hemepeptide (hp). We have chosen the parameters for these systems (Table I) to give a reasonable agreement with the experimental low temperature kinetics.[2] As stated above, the signficant parameters for the recombination kinetics are fx_0^2 and Δ. The individual values of f and x_0 are not determinable and the binding energy has only a minor effect. One should also remember that low temperature experiments sample a limited region of the potential around x_0, where $p^0(x)$ is largest.

The appropriate potentials are shown in Figs. 1 and 2. From these potentials we derive $V^{\ddagger}(x)$, shown in Fig. 3, which is used for calculations in both the frozen and relaxed limits. Temperature effects on the enthalpy and entropy of activation are neglected, an approximation which is probably less justified at higher temperatures where we do not necessarily expect the protein system to be harmonic. In addition, the present model is not meant to account for other processes such as the escape of ligand into solution, which can take place in the relaxed limit. (The effect of such additional states could readily be added to the model.) We have used as simple a potential surface as possible to illustrate most clearly the *kinds* of results which came forth from the model. We have not elaborated the potential to fit the deligation kinetics or the binding enthalpy well, since the theory is insensitive to these parameters. Hence, at high temperatures we expect a qualitative agreement for adequately short times only. Following are the results for the frozen and relaxed cases.

A. Frozen protein coordinate

Distributions of barrier heights [Eqs. (7) and (8)] are shown in Fig. 4. Table II shows the energy of the peaks

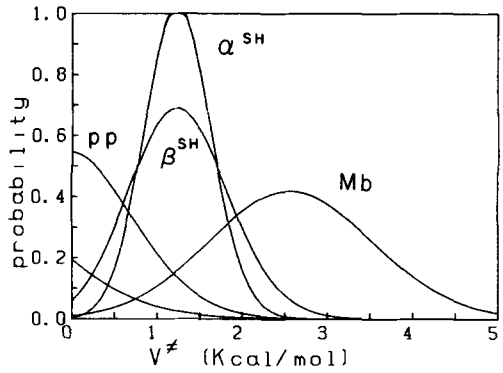

FIG. 4. Distributions of barrier heights, Eqs. (7) and (8). Parameters (D_e, Δ, f, x_0, T_0) from Table I. The unmarked curve is for hemepeptide. The location of the peak is approximately at $V^{\neq}(x_0)$ and its width is determined by the slope of $V^{\neq}(x)$, Fig. 3.

TABLE II. Peak energies $V_p^{\neq}$ for the distributions of barrier heights compared with saddle point energies V^* on the potential surfaces (4) and the Arrhenius activation energy E_A for the lowest eigenvalue λ_0 (calculated at the high D limit from the potentials used to fit the low temperature data).

	$V_p^{\neq}$ [b]				
Heme[a]	Equation (8)	Reference 2	V^{*} [b]	E_A [b]	E_A [b,c]
Mb	2.55	2.39	7.7	7.8	6.3
α^{SH}	1.25	1.10	2.1	2.1	1.8
β^{SH}	1.25	1.03	3.2	3.3	2.6
pp	0	0.24	3.3	3.3	2.4

[a] Abbreviations as in text.
[b] In kcal/mol (1 kcal/mol = 4.184 kJ/mol).
[c] From the approximation (14).

of the distributions. These are usually quite close to the values of Ref. 2, and considerably smaller than the saddle point energies V^* (as measured relative to the energy of the deligated heme) on the potential surfaces [Eq. (4)].

The myoglobin distribution is peaked at the highest energy and is also the widest. The two hemoglobin subunits have comparable peak locations but different widths. This is in qualitative agreement with the distributions suggested in the literature[2(a),2(b)] (except that the latter are less symmetric).

For protoheme Alberding *et al.*[2(c)] postulated an additional faster process I^* to account for the decreased apparent normalization of their rebinding at small times to a number substantially less than unity. We found that this change of normalization occurs naturally within our model without additional suppositions. The distribution shown in Fig. 4 is peaked at zero energy and normalizes to an area of 0.523. The reason that this can happen is clear in Fig. 4. Due to the large distortion (x_0) in the protoheme surface, almost half of the population (all those with $x > \sim 1$ a.u., see Fig. 2) can never cross into the $S=2$ surface, but remains upon photolysis in $S=0$. These molecules do not have a positive barrier for recombination (at least in the present model), and they probably recombine on a much faster time scale.

Figure 5 shows comparison with experiment of the survival probabilities, $Q(t)$ [Eq. (10)], as calculated from the distributions of Fig. 4, and the preexponential factors A, Table I. (The values are quite similar to those of Ref. 2.) No great effort was made to determine a fit beyond that describable as "reasonable agree-

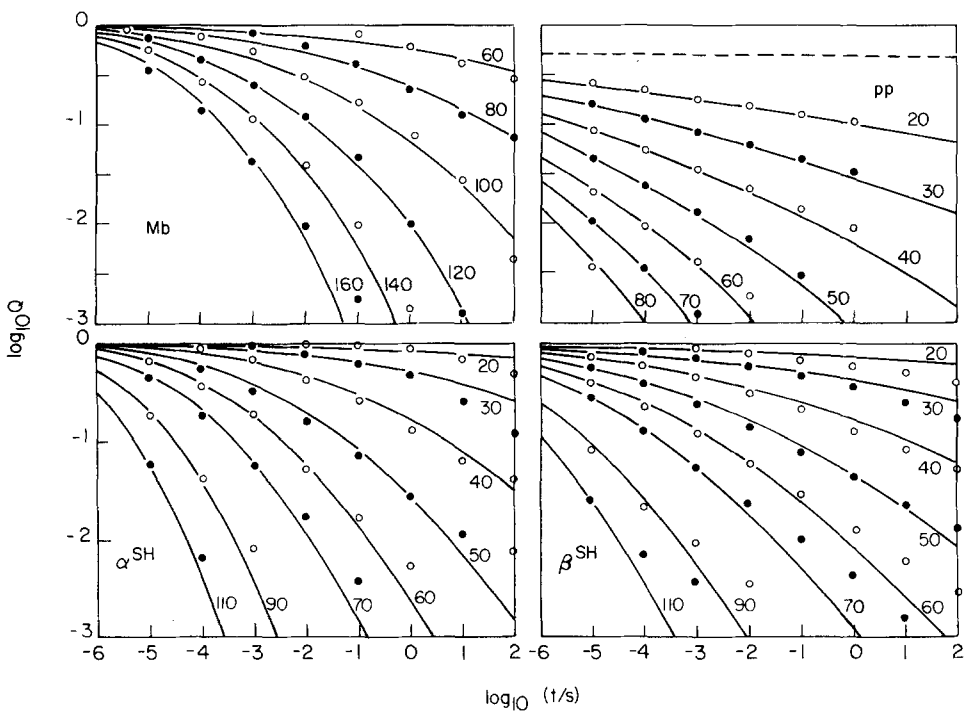

FIG. 5. Low temperature survival probabilities as a function of time (log–log plot). Experimental results, taken from the figures in Ref. 2, are denoted for clarity by alternating close and open circles. (Myoglobin is in 79% glycerol–water. Other solvents as in Ref. 2). Lines are results calculated [Eq. (10)] using the parameters of Table I (which also gives the exact references for the experimental results). Temperatures marked are in degrees K. The $t \to 0$ asymptote for all curves is at $\log Q = 0$, except for protoheme, where it is given by the dashed line.

ment." Recent unpublished experiments (Frauenfelder, private communication) have been carried out at shorter times and lead to different conclusions from those of Alberding *et al.*[2(c)] about entropy distributions. We will analyze the primary data when available. Meanwhile, our protoheme calculation is an example of a new class of behavior which is unified with the others by the model.

Low temperature measurements were also carried out[2(d)] for hemepeptide and carboxymethylated cytochrome *c*. Unlike other results,[2(a)–2(c)] a fast rebinding process was observed[2(d)] in addition to the slower nonexponential process which is common to all systems. The two processes seem to have different spectra.[2(d)] These results were not explained in terms of a distribution of enthalpies and/or entropies, as done for the previously discussed systems.[2(a)–2(c)] In view of our protoheme results, we examine the possibility that the fast component is due to population that cannot cross to the $S=2$ surface (it might be seen in protoheme if experiments are extended to the nanosecond or subnanosecond regime). This is supported by the apparent difference in the spectra.

To check this point we have fitted the slow component for hemepeptide to Eq. (10). The results in Fig. 6 show a semiquantitative agreement. (We were unable to produce a similar agreement for cytochrome *c*). The potential energy surface leading to this fit is even more distorted than that for protoheme (very large x_0), resulting in a peculiar distribution of barrier heights (Fig. 4) normalizing to 0.14. This means that most of the photolyzed population remains in the $S=0$ surface, giving rise to the fast recombination phase (not shown in Fig. 6). The small barrier height for this fast process (which we do not model) has no reason to depend on the protein coordinate, and indeed its kinetics is exponential.[2(d)]

B. Relaxed protein coordinate

Using the numerical procedures of Ref. 13 we have solved the diffusion Eq. (11) for the delegated protein motion (reagents), with $V^{\ddagger}(x)$ of Fig. 3 and an initial

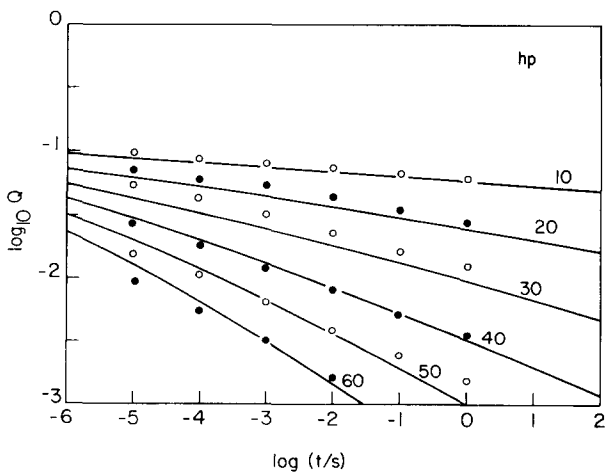

FIG. 6. Same as Fig. 5, for the slow component in CO rebinding to hemepeptide [Ref. 2(d)].

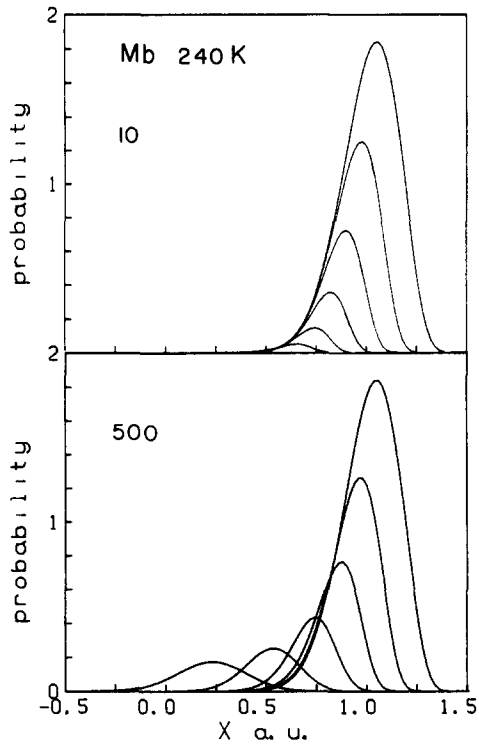

FIG. 7. Probability distribution $p(x,t)$ over protein configurations at different times for Mb–CO at 240 K [direct integration of Eq. (11)]. Times: 1.0×10^{-7}, 6.0×10^{-7}, 2.3×10^{-6}, 7.6×10^{-6}, 2.4×10^{-5}, and 7.7×10^{-5} s. The two panels are for the two marked values of D (in a. u.^{2} s^{-1}).

equilibrium distribution (of the bound precursor) [Eq. (7)]. Since the diffusion coefficient D for protein motion is related to solvent viscosity in an unspecified way we must calculate rebinding curves $Q(t)$ for an array of D values. There is little change for D lower or larger than the minimal or maximal D values shown.

Figure 7 shows the effect of increasing D on the distribution $p(x,t)$. For small D it is consumed by the ligation reaction where $k(x)$ is large. At larger D, diffusion carries the distribution downhill (until it becomes peaked above the minimum of the potential well, at $x=0$), away from large $k(x)$, resulting in slower decay.

Figure 8 demonstrates a central feature of the present theory, that it is able to make use of the low temperature data [in the form of the potential $V(r,x)$] for explaining results in the high temperature range, in qualitative agreement with the lower panel of Fig. 1, Ref. 2(e). As D increases, the curves follow the frozen-limit curve for a shorter time, then level off and finally decay exponentially. The time constants for the longest-time exponential decay should *not* be compared. Hence allowing the protein to adjust its configuration *slows down* the rebinding in the intermediate time range. Many will find this result counterintuitive. Others have assumed[2] that the innermost barrier at high temperatures is equal to the peak in the low temperature distribution of barrier heights $V_p^{\ddagger}$. The physical reason that this assumption need not hold is clear. Since the state just before the flash has Mb–CO ligated, the initial

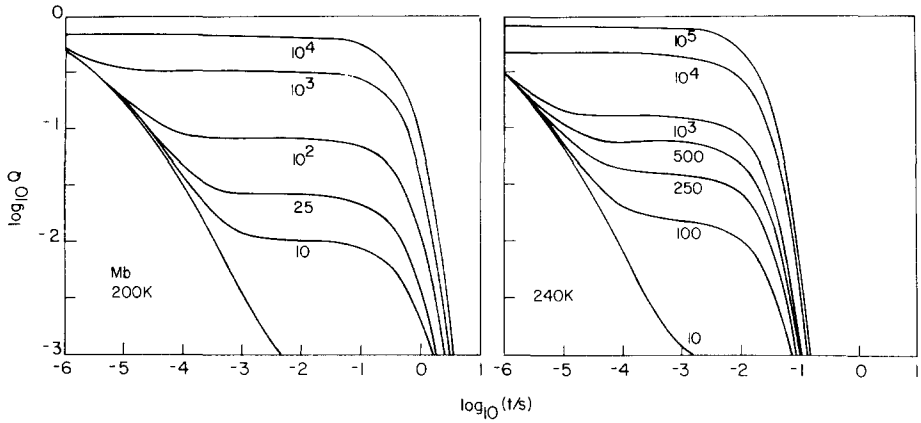

FIG. 8. Survival probability rebinding curves [Eq. (12)] for Mb–CO at two higher temperatures. Each curve is for a different D value (in a. u.^{2} s^{-1}). Curves for two lowest values—by direct integration, the other—by the eigenvalue method (Ref. 13).

protein configuration is such as to make this a low energy state. This configuration also pertains just after the flash. At this time, recombination is still relatively favorable for the protein configuration is still like that of the bound state (product configuration). In a short time, however, the protein relaxes to stabilize the unligated state (reagent state) and the recombination is then less favorable.

The results of Fig. 8 suggest that a leveling off (change in slope) of $Q(t)$ does not necessarily point to an additional *sequential* process of CO transfer from another site in the protein to the heme pocket (barriers in series).[2] Even for a single process (geminate recombination) one may observe such an effect, resulting from diffusion perpendicular to the reaction coordinate (reaction has many *parallel* paths from different configurations). $Q(t)$ levels off once the distribution reaches the bottom of the reagents' well, and the kinetics changes from power law to exponential. We do not mean to imply that no sequential steps other than escape into solution occur. But the total logical consequences of the innermost barrier distribution need to be evaluated before postulating additional series kinetic processes on the basis of kinetic data alone.

Theory and experiments disagree at long times. The final exponent in Fig. 8, λ_0, is almost independent of D [cf. Eqs. (13) and (14)], while the experimental populations survive much longer and decay with different rates. This difference, apparent after a few milliseconds, is due in part to the escape of CO to solution, which is not included in the present simulation. Frauenfelder (private communication) found that correction for solvent escape would lead to a plateau which is not flat, but falls slowly at about $t^{-1/2}$ up to $T = 300$ K. A power law dependence in this temperature range could imply the existence of other incomplete configurations averaging even at the higher temperatures, a possibility our modeling does not contemplate. Alternatively, bimolecular kinetics are not always simple, and the correction for solvent escape is not necessarily unambigous. The *development of the plateau* in Fig. 8 is a consequence of the diffusional motions, whether the long-time cutoff is geminate recombination *or* recombination from solution.

Even for shorter times, results in Fig. 8 do not agree quantitatively with experiment. In particular, the time scale for the change in slope in $Q(t)$ mentioned above, is too short in comparison with experiment.[2(e)] Indeed, the low temperature results carry chiefly information on the r dependence, of the potential, and are rather insensitive to the x dependence. In particular, since the initial distribution is centered away from the minimum of the deligated heme potential at $x = 0$, low temperature results do not probe that part of the potential. Any function of x alone, which is independent of the spin state, can be added to $V(r, x)$ without changing $V^{\ddagger}(x)$. This would result in a small change in the low temperature kinetics (due to a variation in the initial distribution), but may alter appreciably the minimum in the surface, the high temperature stochastic dynamics along the protein coordinate and in the high temperature limit the activation enthalpy of rebinding. These uncertainties do not affect the qualitative conclusion of the model as discussed above, namely, that the barrier to recombination increases with time.

Recent room temperature measurements[4(d)] of CO rebinding kinetics to Mb in the nanosecond regime, are also in quantitative disagreement with the extension of Fig. 8 to 300 K (not shown). The experiment[4(d)] shows a seemingly exponential decay of unbound Mb, which levels off after about 200 ns at 4% recombination. It is unclear to us whether this is a continuation of the trend in Fig. 8 and due to a changeover from multi to monoexponential geminate recombination, or [as interpreted in Ref. 4(b)] due to a transition from geminate (exponent λ_0) to bimolecular recombination from solution. Additional experimental and theoretical work is needed to answer these questions.

In another recent experiment,[2(f)] it was found that as the pH is decreased from 7 to 5, the peak in the low temperature distribution of barrier heights decreases (by about 0.5 kcal/mol for Mb–CO), and the high temperature exponent (λ_0 in our notation) increases (by about a factor of 3 for Mb–CO at 300 K). By decreasing the parameter Δ and x_0, we were able to achieve a good fit to low temperature results at pH 5. Since different choices of the parameters result in variations in the fit that are smaller than the difference between

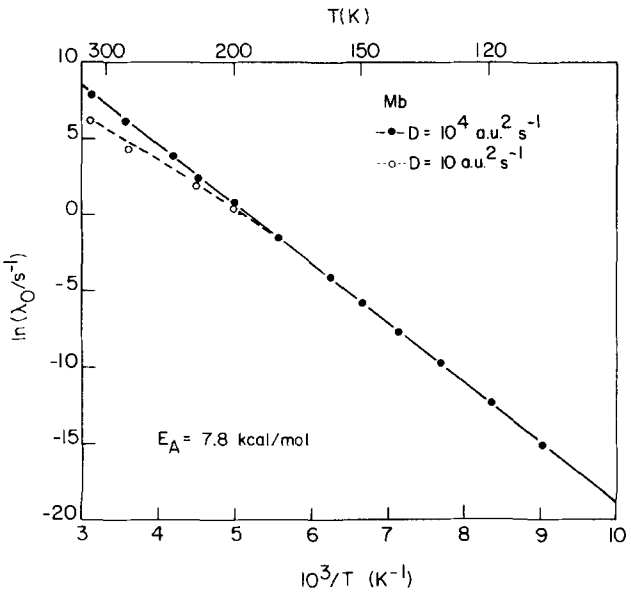

FIG. 9. Temperature dependence of lowest eigenvalue λ_0 for Mb–CO, for two diffusion coefficients. For large D it is a perfect Arrhenius plot, with an activation energy of 7.8 kcal/mol and a preexponent exactly the same as that of $k(x)$ [A in Table I]. The calculated points are connected by lines to guide the eye.

the two Mb–CO measurements,[2(e),2(f)] we could only determine the shift in the distribution's peak to be in the range 0.3–0.6 kcal/mol and that the ratio $\lambda_0(p\text{H } 5)$. $\lambda_0(p\text{H } 7)$ should lie in the range 2–20 at 300 K.

The temperature dependence of the lowest eigenvalue λ_0 as calculated from the Mb–CO potential energy surface, it shown in Fig. 9. At large D it is a perfect Arrhenius curve, in agreement with Eq. (13), though the activation energy is somewhat different from that suggested by the approximate Eq. (14) (see Table II). The temperature dependence of λ_1 is shown in Fig. 10. When D is large it deviates slightly (at high temperatures) from a straight line [Eq. (15)] and considerably when D is small.

The other heme systems have smaller barriers to geminate CO recombination and their high temperature survival probability plots are therefore in the nanosecond regime, as seen in Fig. 11. (This is perhaps the reason that only three consecutive barriers were identified[2] for these systems as opposed to four in Mb. As stated above, we believe that perhaps one of the "processes" in Mb is due to effects of diffusion perpendicular to the reaction coordinate). Kinetic experiments in this time regime have not been so extensive. Available experimental results for human hemoglobin[4(a)–4(c)] indicate 30%–50% recombination within 100 ns of (room temperature) photolysis. The results of Fig. 11 suggest that this is due mainly to the β subunit. The results for protoheme (Fig. 11) show that all the observable unbound population [in upper panel of Fig. 1 of Ref. 2(e)] is due to CO that has escaped into solution. This process would typically take a few nanoseconds in protoheme, as opposed to a few milliseconds in Mb.

The effect of temperature variations is through the initial distribution width, $k(x)$, and D. Calculations explicitly include all effects of temperature on the first two (except for T dependence of enthalpy and entropy of activation). The diffusion constant would presumably increase with T in an Arrhenius fashion or faster if a glass transition is being approached. The short time rebinding curve for α^{SH} at 200 K is likely to be one of

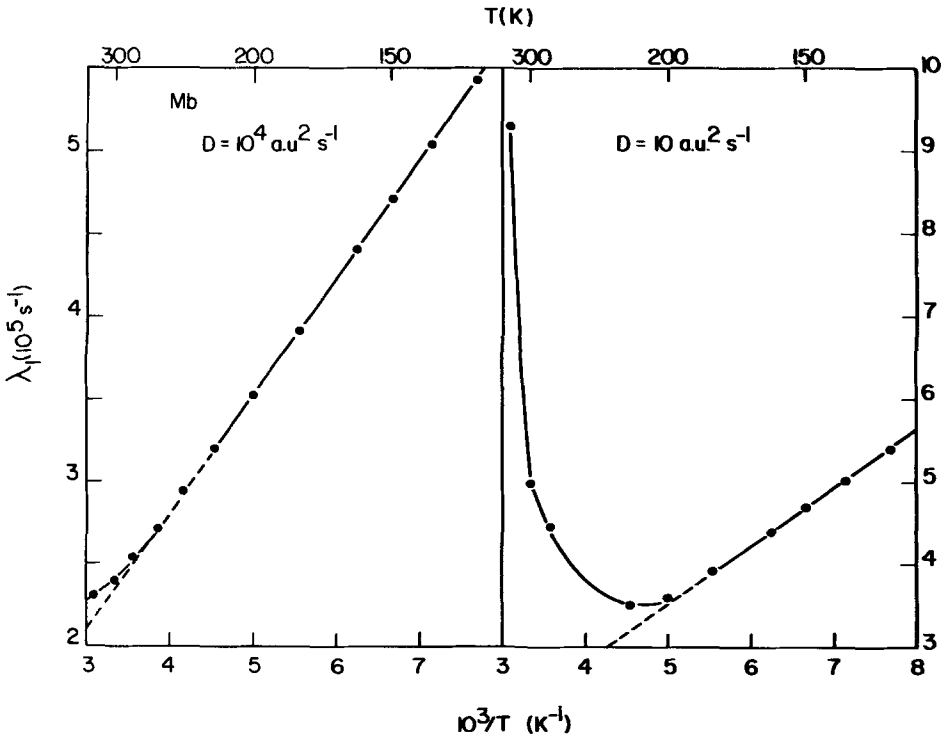

FIG. 10. Temperature dependence of λ_1 for Mb–CO, for two diffusion coefficients. Straight dashed line is Eq. (15). The calculated points are connected by lines to guide the eye.

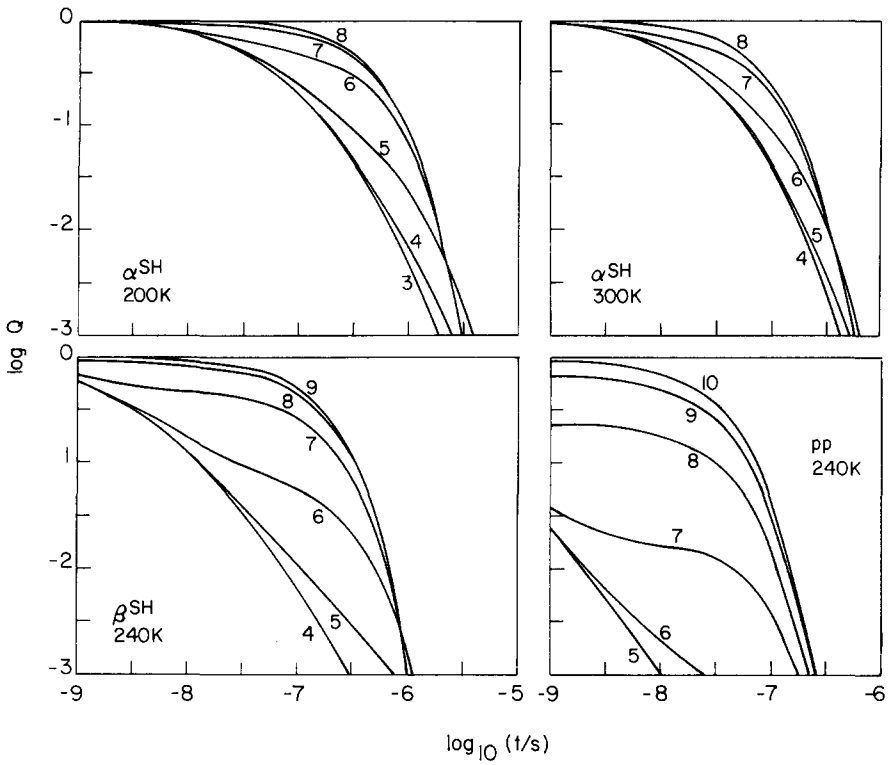

FIG. 11. Same as Fig. 8, for other heme proteins, the numbers are $\log_{10} D$ (D in a. u.^{2} s^{-1}).

the small D curves in (the upper left panel of) Fig. 11, whereas at 300 K it is likely to follow a curve of higher D (but with an exponent which reflects the rate constant for recombination from solution). This again results in a transition from power law to exponential kinetics with increasing temperature, in qualitative agreement with the short time behavior in the left panels of Fig. 1 of Ref. 2(b).

The Arrhenius activation energy for λ_0 [cf. Eq. (13)], E_A for all four heme systems is given in Table II. In all cases, the preexponent A is the same as that in $k(x)$. There are three features to note. First, Eq. (14) gives a first order approximation which is helpful as an initial guess for λ_0. Second, E_A is the same as the saddle point energy for the appropriate potential energy surface of Fig. 2 (measured relative to the reagents' well). Finally, E_A is always considerably larger than the energy of the peak in the distribution of barrier heights $V_p^{\ddagger}$. This result is again a consequence of the relaxation of the protein to a reactant-favoring configuration. (In an analysis[2] of the high temperature results E_A was assumed equal to $V_p^{\ddagger}$.)

C. Dependence on initial conditions: A new experiment

In the example for intramolecular electron transfer[13] the effect of varying the initial conditions was investigated by choosing initial distributions with peaks displaced relative to the minimum in the potential. The examples shown so far correspond to "negative displacements" (Figs. 4 and bottom panels of Fig. 6 in Ref. 13), where the peak is initially displaced in direction of increasing $k(x)$. An alternative preparation of the initial distribution is, in principle, possible by allowing the sample to equilibrate in light of intensity and wavelength appropriate to keep the heme deligated. The initial distribution would now peak at $x=0$ ("zero displacement"). The reaction would be initiated by turning the light off.

The results presented below utilize the same methods as above only replacing $x-x_0$ in Eq. (7) by x. Even the eigenvalues do not change, as they are independent of initial conditions. Figure 12 shows the new distributions of barrier heights for the heme subunits. They are shifted to higher energies and somewhat widened, be-

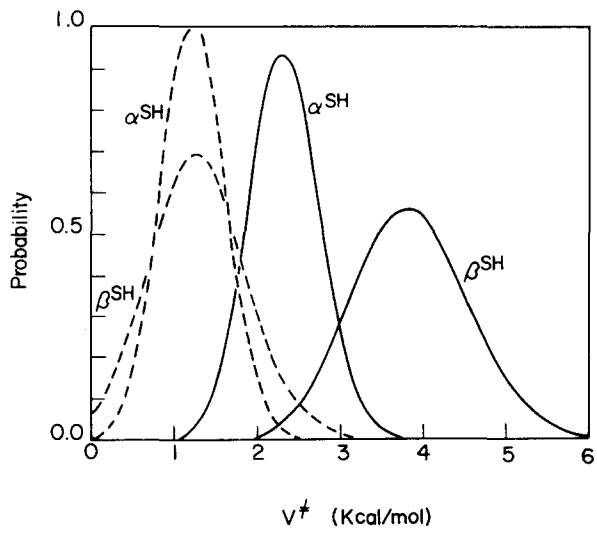

FIG. 12. Distributions of barrier heights for an alternative preparation of the initial population by a very long laser pulse. Dashed lines are previous results (Fig. 4).

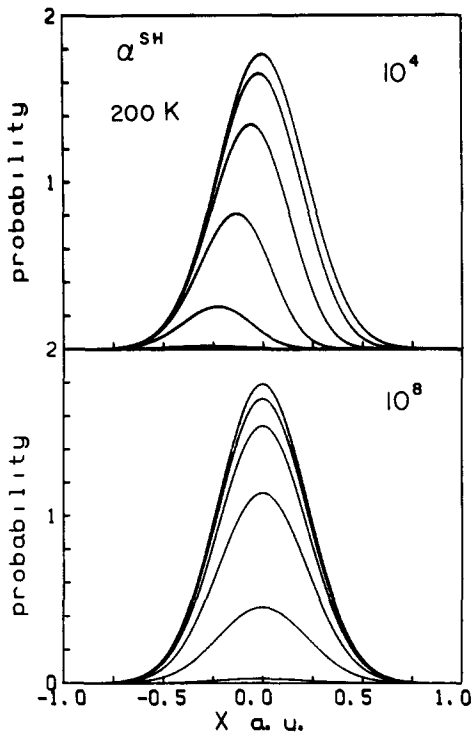

FIG. 13. Same as Fig. 7 for the alternative preparation of the initial population upper curves ($D=10^4$ a.u.^{2} s^{-1}), by direct integration at $t=1.0\times10^{-8}$, 6.0×10^{-8}, 2.3×10^{-7}, 7.6×10^{-7}, 2.4×10^{-6}, and 7.7×10^{-6} s. Lower curves ($D=10^8$ a.u.^{2} s^{-1}) by the eigenvalue method at $t=0$, 2.1×10^{-8}, 6.3×10^{-8}, 1.9×10^{-7}, 5.8×10^{-7}, and 1.7×10^{-6} s.

cause they now peak at $x=0<x_0$, and $V^{\ddagger}$ increases with decreasing x (Fig. 3).

Figure 13 shows $p(x,t)$ for α heme for two values of D. Here diffusion causes the peak to move back to $x=0$, *towards* large $k(x)$, as opposed to the cases discussed above when the peak moved away from large $k(x)$. Therefore, decay would be faster for larger D.

This is seen also in the results for $Q(t)$, Fig. 14. The frozen-limit ($D=0$) populations survive longer (compared to the populations in Fig. 5), whereas increasing D results in faster decay. This is just the opposite of the situation of Fig. 11, and is due to the fact that now diffusion replenishes the population of configurations with large $k(x)$. The above conclusions still wait experimental verification.

The two different behaviors can be achieved by a short vs long period of light preceding recombination. For pulses of intermediate length, one may expect some intermediate behavior. It is therefore important to investigate the dependence of kinetics on pulse duration when the protein coordinate may adjust during a pulse.

D. Direct experimental probe of protein coordinate distributions

Because many properties of the protein may depend on the coordinate x, experiments which can follow the putative changes in the protein coordinate are possible. For example, if the frequency of a heme vibrational mode depends on x, the remaining deoxy hemes in a flash photolysis experiment will have a time dependent Raman scattering from this mode. Such effects were observed for hemoglobin,[18] where they are complicated by subunit inequivalence and slow quaternary structure changes. Indeed, in a case in which the shift is proportional to x and the intrinsic line width is narrow, the observed Raman line shape should be a faithful monitor of the shape of $p(x,t)$ (with a scaled ordinate and abscissa).

The above should be true both for $D=0$ and when D is finite and significant. The faithfulness of this representation depends only on the linearity and narrow linewidth suppositions, and is independent of knowing the details of $V(r,x)$. When these suppositions are not true, or when the available monitor of structural change is less easily characterized (e.g., an absorbance change at a

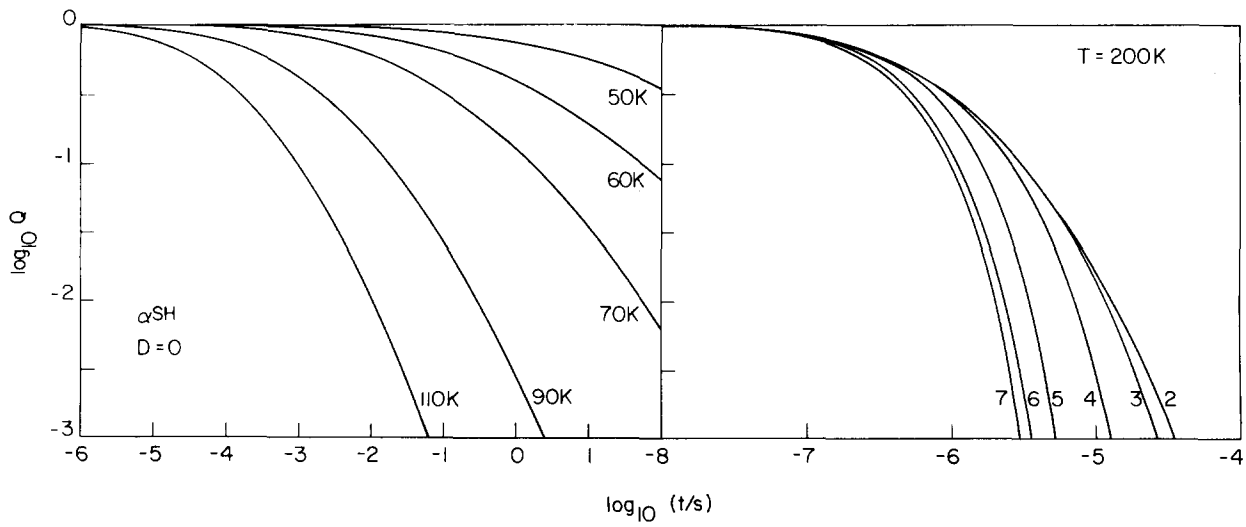

FIG. 14. Survival probability plots for α heme for the alternative preparation of the initial distribution. Left panel: Low temperatures, zero diffusion. Right panel: At 200 K for different values of $\log_{10} D$.

particular wavelength), theoretical calculations of the time dependence of the deoxy state can still be compared to experiments, though less directly. In such cases, we expect the time dependence of effects to resemble that of the average value of the coordinate $\langle x \rangle$, cf. Fig. 5 in Ref. 13. Studies on such structural probes could provide the most significant examination of the structural basis for the theory.

IV. CONCLUSION

A model for the dependence of barrier height on protein coordinate has been used to analyze the low temperature CO binding to heme proteins. The model is based on a potential energy surface constructed from the intersecting surfaces for the two iron spin states. The model demonstrates how the stress of the protein or solvent on the porphyrin ring can give rise to a distribution of barrier heights, which one can fit quantitatively to the low temperature ("frozen") kinetics. According to this model, it is possible for some of the population not to cross from one spin surface to the other. This portion of the population does not participate in the observed kinetics (their recombination is probably much faster and their spectrum different), resulting in distributions of barrier heights normalizing to less than unity. This is observed experimentally for protoheme.

The theory of bounded diffusion perpendicular to the reaction coordinate[13] has been used to follow the kinetics under "relaxed" conditions of high temperatures or low viscosities, when protein motion is possible. The coupling of diffusion and reaction was seen to give rise to quite elaborate kinetic curves, changing from power law in the frozen limit to exponential in the relaxed limit. For intermediate diffusion constants, the rebinding curves change slope when the rebinding kinetics change from frozen at short times to relaxed at long times. Hence, such a change in slope need not necessarily be attributed[2] to additional barriers in "sequential" kinetics. It is a natural consequence of "parallel" kinetics coupled with diffusion.

In contrast to diffusion along the reaction coordinate[5] which goes to zero with decreasing D, reaction rates do not vanish for high viscosity when diffusion is perpendicular to the reaction coordinate,[13] hence, "non-Kramers kinetics"[2,11] follows most naturally. The overall dependence on D is better discussed in terms of the "average survival time" $\langle \tau \rangle$ than in terms of an exponent such as λ_0, because for small D many exponents contribute to $Q(t)$. For D which is not extremely large, $\langle \tau \rangle$ was seen[13] to be proportional to a constant plus a power of D.

Another assumption in the literature[2] is questioned here, for in our theory the activation energy for large D exponential kinetics can be significantly larger than the peak in the $(D=0)$ distribution of barrier heights.

We believe there are good physical reasons for the relevance of such theoretical considerations to some problems in ligand binding kinetics, and therefore analyzed the heme-CO recombination in detail to display the wealth of effects the theory is capable of producing. But we should emphasize, that many of the details to which we give bounded diffusion interpretations might in any particular system be due to such concatenations of details as are postulated in Refs. 2(a)–2(f).

Fortunately, there are some predictions of the new point of view which are not obvious concomitants of other viewpoints. The first involves measuring kinetics from an alternative initial distribution prepared by a long light pulse prior to recombination. Second, the study of structural probes of unligated hemes during the recombination process forms a critical test of the theory. Indeed, under some simplifying but not impossible suppositions, the form of the basic conceptual function $p(x,t)$ can be *directly* measured in transient resonant Raman scattering.

ACKNOWLEDGMENTS

The authors wish to thank R. H. Austin, L. Eisenstein, H. Frauenfelder, J. M. Friedman, and D. L. Rousseau for helpful correspondence and discussions.

[1] E. Antonini and M. Brunori, *Hemoglobin and Myoglobin in their Interaction with Ligands* (North–Holland, Amsterdam, 1971).

[2] (a) R. H. Austin, K. W. Beeson, L. Eisenstein, H. Frauenfelder, and I. C. Gunsalus, Biochemistry **14**, 5355 (1975); (b) N. Alberding, S. S. Chan, L. Eisenstein, H. Frauenfelder, D. Good, I. C. Gunsalus, T. M. Nordlund, M. F. Perutz, A. H. Reynolds, and L. B. Sorensen, *ibid.* **17**, 43 (1978); (c) N. Alberding, R. H. Austin, S. S. Chan, L. Eisenstein, H. Frauenfelder, I. C. Gunsalus, and T. M. Nordlund, J. Chem. Phys. **65**, 4701 (1976); (d) N. Alberding, R. H. Austin, S. S. Chan, L. Eisenstein, H. Frauenfelder, D. Good, K. Kaufmann, M. C. Marden, T. M. Nordlund, L. Reinisch, A. H. Reynolds, L. B. Sorensen, G. C. Wagner, and K. T. Yue, Biophys. J. **22**, 319 (1978); (e) D. Beece, L. Eisenstein, H. Frauenfelder, D. Good, M. C. Marden, L. Reinisch, A. H. Reynolds, L. B. Sorensen, and K. T. Yue, Biochemistry **19**, 5147 (1980); M. C. Marden, Ph.D. thesis, University of Illinois, Urbana, Illinois, 1981; (f) W. Doster, D. Beece, S. F. Bowne, E. E. DiIorio, L. Eisenstein, H. Frauenfelder, L. Reinisch, E. Shyamsunder, K. H. Winterhatter, and K. T. Yue, Biochemistry **21**, 4831 (1982).

[3] B. B. Hasinoff, J. Chem. Phys. **82**, 2630 (1980); **85**, 526 (1981).

[4] (a) D. A. Duddell, R. J. Morris, and J. T. Richards, Biochim. Biophys. Acta **621**, 1 (1980); D. A. Duddell, R. J. Morris, N. J. Muttucumaru, and J. T. Richards, Photochem. Photobiol. **31**, 479 (1980); (b) B. Alpert, S. El Mohsni, L. Lindqvist, and F. Tfibel, Chem. Phys. Lett. **64**, 11 (1979); (c) J. M. Friedman and K. B. Lyons, Nature (London) **284**, 574 (1980); (d) E. R. Henry, J. H. Sommer, J. Hofrichter, and W. A. Eaton, J. Mol. Biol. (in press).

[5] (a) H. Kramers, Physica (Utrecht) **7**, 289 (1940); (b) S. Chandrasekhar, Rev. Mod. Phys. **15**, 1 (1943).

[6] (a) H. Frauenfelder, G. A. Petsko, and D. Tsernoglou, Nature (London) **280**, 558 (1979); H. Frauenfelder and G. A. Petsko, Biophys. J. **32**, 465 (1980); (b) E. R. Bauminger, S. G. Cohen, I. Nowik, S. Ofer, and J. Yariv, Proc. Natl. Acad. Sci. USA 80, 736 (1983); E. W. Knapp, S. F. Fischer, and F. Parak, J. Chem. Phys. **78**, 4701 (1983).

[7] D. A. Case and M. Karplus, J. Mol. Biol. **132**, 343 (1979).

[8] N. Alberding, H. Frauenfelder, and P. Hanggi, Proc. Natl. Acad. Sci. USA **75**, 26 (1978); P. Hanggi, J. Theor. Biol. **74**, 337 (1978).

[9]J. Jortner and J. Ulstrup, J. Am. Chem. Soc. **101**, 744 (1979).
[10]D. Peak, J. Chem. Phys. **76**, 3792 (1982).
[11]B. Gavish, Phys. Rev. Lett. **44**, 1160 (1980).
[12]M. Mangel, J. Chem. Phys. **75**, 5969 (1981).
[13]N. Agmon and J. J. Hopfield, J. Chem. Phys. **78**, 6947 (1983).
[14]H. Eicher, D. Bade, and F. Parak, J. Chem. Phys. **64**, 1446 (1976).
[15]W. A. Goddard III and B. D. Olafson in *Biochemical and Clinical Aspects of Oxygen*, edited by W. D. Caughey (Academic, New York, 1979), p. 87, and references therein; B. D. Olafson, Ph. D. thesis, California Institute of Technology, Pasadena, CA, 1978.
[16]M. H. Redi, J. J. Hopfield, and B. S. Gerstman, Biophys. J. **35**, 471 (1981); B. S. Gerstman, R. H. Austin, and J. J. Hopfield, Phys. Rev. Lett. **47**, 1636 (1981); B. S. Gerstman, Ph. D. thesis, Princeton University, Princeton, NJ, 1981.
[17]J. L. Hoard and W. R. Scheidt, Proc. Natl. Acad. Sci. USA **70**, 3919 (1972); L. J. Radonovich, A. Bloom, and J. L. Hoard, J. Am. Chem. Soc. **94**, 2073 (1972); J. P. Collman, N. Kim, J. L. Hoard, G. Lang, L. J. Radonovich, and C. A. Reed, in Abstracts of the 167th Meeting of the American Chemical Society, Los Angeles, 1974, INOR 29.
[18]T. W. Scott, J. M. Friedman, M. Ikeda-Saito, and T. Yonetani, J. Am. Chem. Soc. (submitted).